AMERICAN SOCIETY of
GENE & CELL
THERAPY

A High-Throughput Screening Identifies MicroRNA Inhibitors That Influence Neuronal Maintenance and/or Response to Oxidative Stress

Joan Pallarès-Albanell,[1,7] M. Teresa Zomeño-Abellán,[1,7] Georgia Escaramís,[1,2,3,4] Lorena Pantano,[5] Aroa Soriano,[6] Miguel F. Segura,[6] and Eulàlia Martí[1,2,3,4]

[1]Centre for Genomic Regulation (CRG), The Barcelona Institute for Science and Technology, Dr. Aiguader 88, Barcelona 08003, Spain; [2]Departament de Biomedicina, Facultat de Medicina i Ciències de la Salut, Institut de Neurociències, Universitat de Barcelona, Barcelona 08036, Spain; [3]Research Group on Statistics, Econometrics and Health, Universitat de Girona, 17003, Girona, Spain; [4]Centro de Investigación Biomédica en Red de Epidemiología y Salud Pública (CIBERESP), Ministerio de Ciencia Innovación y Universidades, Madrid, Spain; [5]Bioinformatics Core, Department of Biostatistics, Harvard T.H. Chan School of Public Health, Boston, MA 02115, USA; [6]Group of Translational Research in Child and Adolescent Cancer, Vall d'Hebron Research Institute (VHIR), Universitat Autònoma de Barcelona (UAB), Passeig Vall d'Hebron 119, Barcelona 08035, Spain

Small non-coding RNAs (sncRNAs), including microRNAs (miRNAs) are important post-transcriptional gene expression regulators relevant in physiological and pathological processes. Here, we combined a high-throughput functional screening (HTFS) platform with a library of antisense oligonucleotides (ASOs) to systematically identify sncRNAs that affect neuronal cell survival in basal conditions and in response to oxidative stress (OS), a major hallmark in neurodegenerative diseases. We considered hits commonly detected by two statistical methods in three biological replicates. Forty-seven ASOs targeting miRNAs (miRNA-ASOs) consistently decreased cell viability under basal conditions. A total of 60 miRNA-ASOs worsened cell viability impairment mediated by OS, with 36.6% commonly affecting cell viability under basal conditions. In addition, 40 miRNA-ASOs significantly protected neuronal cells from OS. In agreement with cell viability impairment, damaging miRNA-ASOs specifically induced increased free radical biogenesis. miRNAs targeted by the detrimental ASOs are enriched in the fraction of miRNAs downregulated by OS, suggesting that the miRNA expression pattern after OS contributes to neuronal damage. The present HTFS highlighted potentially druggable sncRNAs. However, future studies are needed to define the pathways by which the identified ASOs regulate cell survival and OS response and to explore the potential of translating the current findings into clinical applications.

INTRODUCTION

Different classes of small non-coding RNA (sncRNA) species have been uncovered with sequencing strategies, with many modulating gene expression through diverse mechanisms. MicroRNAs (miRNAs) are the best known class of sncRNAs, transcribed as long precursors (pri-miRNAs) and processed to a mature, double-stranded, short RNA of ~20–25 nt.[1] The active strand of this duplex is loaded into the RNA-induced silencing complex (RISC), where it guides mRNA

decay or inhibition of translation through incomplete base pairing with the 3′ UTR of target genes.[2] Each miRNA targets hundreds of genes, and a gene can be targeted by several miRNAs.[3] We have recently shown that the number of miRNAs is larger than anticipated,[4] with new miRNA candidates being evolutionarily young and overrepresented in the human brain.

Relative to other tissues, the nervous system is especially enriched in diverse miRNAs and other types of ncRNAs of unknown function that show specific spatial-temporal patterns of expression.[5] Functional studies, with special emphasis on miRNAs, have revealed that their dynamic expression has essential roles in cell-type specification and differentiation during development,[6] but also in the maintenance of adult post-mitotic cells. Conditional inactivation of Dicer, the limiting enzyme of miRNA biogenesis, in specific areas of the adult mouse brain consistently results in progressive loss of specific types of neurons.[7–9] In addition, perturbation of selective miRNAs affects neuronal viability.[10–12] Therefore, specific miRNAs and possibly other types of sncRNAs may be particularly relevant in preserving neuronal viability.

sncRNA expression is highly sensitive to physiological and pathological stimuli, with consequent modifications in gene expression leading to a specific cell status. In neurodegenerative diseases, ncRNA alterations occurring at prodromal phases are especially relevant, as they may determine initial gene expression changes with pathogenic impact. This scenario prompts the idea that the activity of specific sncRNAs could be targeted to overcome or delay pathogenesis.
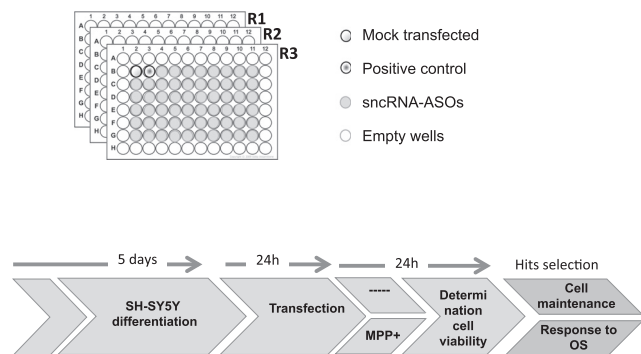
Figure 1. Scheme of the Experimental Design for the HTFS

Stable, chemically modified antisense oligonucleotides complementary to miRNAs (miRNA-ASOs) bind with high specificity to the target sncRNAs and inhibit their activity by impeding the association of miRNAs with the complementary sites in the target mRNAs, which may restore expression levels of specific genes. miRNA-ASOs are therefore useful molecules for identifying miRNAs with a relevant role in neuronal maintenance. Stabilized ASOs targeting other classes of sncRNA (sncRNA-ASOs) have the potential to similarly uncover the novel bioactive species implicated in cell survival.

High-throughput functional screenings (HTFSs) have used miRNA-ASOs or RNA molecules designed to mimic endogenous mature miRNA (miRNA-mimics), to identify species with an effect in the expression of dosage-sensitive genes, in reporter assays.[13,14] In addition, most HTFS analyses have evaluated the effect of a moderate number of miRNA-mimics or -ASOs in tumorigenic outcomes, including cell invasiveness,[15] tumor cell death,[16] or cell growth.[17,18] HTFS studies to generally identify sncRNAs with a role in differentiated neuronal cell viability are missing. In the present study, we developed a high-throughput screening platform to evaluate the effect of 2,004 sncRNA-ASOs, targeting miRNAs (a total of 1,954) and non-miRNA sncRNAs (a total of 50) in neuronal cell viability, under both normal and basal conditions and following oxidative stress (OS), a major hallmark in neurodegenerative disorders. We used a statistical scoring method developed for high-throughput screenings to target hits,[19] a subgroup of which was confirmed by using an alternative statistical strategy that we developed, dealing with biological replicates. In addition, we used alternative functional approaches to validate hits targeted by both statistical methods. Our approach has identified a reliable group of detrimental and protective sncRNA-ASOs, which may reflect the involvement of the targeted species in neuronal maintenance and response to stress. Finally, we analyzed sncRNA expression dynamics after OS, suggesting that deregulation of several sncRNA species may contribute to neuronal dysfunction. Our data provide a large catalog of sncRNA-ASOs that may be selected for pre-clinical validation in model organisms.

RESULTS

HTFS Identifies Multiple miRNA-ASOs That Affect Cell Viability and Response to MPP+ Stress

To identify sncRNAs with a role in neuronal survival, we set up an HTFS to evaluate cell viability after inhibiting the activity of miRNAs and other types of sncRNAs. We used a library of locked-nucleic-acid (LNA)-modified ASOs targeting 1,954 miRNAs and 50 sncRNAs not typified as miRNAs that our studies have described in deep-sequencing data analysis of human brain samples[20] (Table S1). The sncRNA-ASOs were individually transfected in three independent biological replicates into SH-SY5Y cells differentiated into a post-mitotic, dopaminergic phenotype, a cell model largely used to understand the molecular bases of neuronal dysfunction.[21,22] Two days after transfection, viability was determined with WST-1 tetrazolium reagent, whose bioreduction correlates with the number of metabolically active cells[23] (Figure 1). In every plate, we included a mock-transfected condition and a positive control of decreased cell viability, by transfecting a sncRNA-ASO that induces cell death.

We used two statistical approaches to identify sncRNA-ASOs that affect neuronal cell viability. The first approach is based on the B score,[19] a powerful method designed for plate-based assays that detects hits under the assumption that the vast majority of the screened sncRNA-ASOs are not active. Statistical B scores are constructed based on the observation that hits behave as outliers compared to the majority of non-effective sncRNAs-ASOs. The normalized B scores follow a standardized Gaussian distribution, so that outliers, our potential hits, can be defined as values below −2. A positional effect was detected, with B score values in close columns or rows clustering together (Figure S1). As indicated in the B score method, we applied an iterative median polished that robustly avoids position-related systematic errors.[12]

We consistently detected a decrease in cell viability in wells transfected with the positive control sncRNA-ASO (Figure 2). A significant enrichment of hits was detected among the sncRNAs expressed in our model system (Figure S2), which agrees with a specific effect of the ASOs on sncRNAs present in differentiated neuronal cells, thus favoring the detection of true detrimental effects. Among the sncRNAs (988 miRNAs and 9 sncRNAs) with mean normalized counts >1, according to sequencing analysis (Table S2), a total of 76 sncRNA-ASOs targeting miRNAs (miRNA-ASOs) significantly decreased viability in differentiated SH-SY5Y (B score <−2), in at least two biological replicates (Table 1).

The second statistical approach is based on a linear mixed effects model (LMM) that accounts for the three biological replicates as another source of variability in the experimental design. Similar to the B score method, the LMM uses the bulk of data as self-controls and accounts for systematic biases. The fact that the experimental design includes biological triplicates per sample, allows us to include sample random effects in the model so that outliers or candidate hits
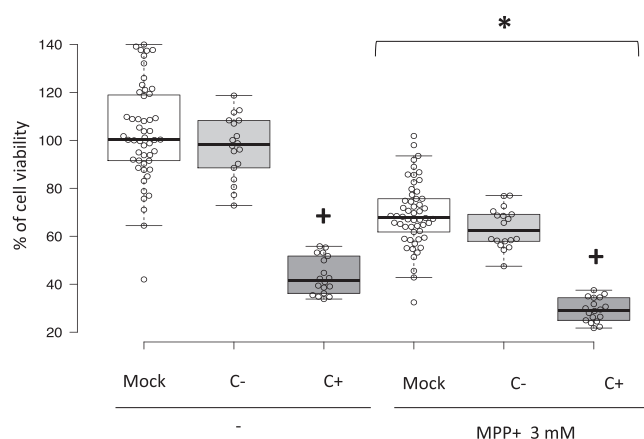
Figure 2. Cell Viability Determinations in the HTFS under Basal Conditions and in Response to Oxidative Stress

Cell viability determinations in every plate are shown in mock-transfected cells, cells transfected with a negative control sncRNA-ASO (C−), and cells transfected with the positive control sncRNA-ASO (C+), under basal conditions and following treatment with 3 mM MPP+. Each dot represents the percentage of cell viability determinations in a well, with 100% considered to be the mock-transfected cells under basal conditions. All values are represented relative to a mock-transfected well under basal conditions. Differences between conditions were determined by using linear mixed-effects models, where experimental conditions to be compared are included in the model as fixed affects, and plates are included as random effects to account for between-plate variability. A Bonferroni correction was applied to account for multiple comparisons (number of comparisons = 9). Significant differences are found between MPP+ treatment and basal conditions, in each experimental condition (Mock, C−, and C+; *p < 0.001), and in C+ versus mock and C− under basal conditions and after exposure to MPP+ (+p < 0.001).

are summarized in a single value. This model provided a total of 87 sncRNA-ASOs that decreased cell viability, of which 47 (54%) were coincidental with the B score-based approach (Table 1). These data suggest that the 47 sncRNAs targeted by the correspondent ASOs participate in the maintenance of cell viability. According to the miRNA enrichment analysis and annotation (miEAA) tool,[24] the pathways targeted by the group of miRNAs whose ASOs decrease cell viability include *nervous system development*, *apoptosis*, and *DNA damage response* and pathways associated with diverse neurodegenerative conditions, including Parkinson's and Huntington's diseases (Table S3).

An independent HTFS was performed to evaluate the effect of sncRNA-ASOs in cell viability after a stressful stimulus (Figure 1). Differentiated SH-SY5Y cells were transfected with the sncRNA-ASOs, and 24 h later, they were subjected to 1-methyl-4-phenylpyridinium (MPP+) stress for an additional 24 h, after which cell viability was determined. MPP+ impairs oxidative phosphorylation in mitochondria by inhibiting complex I, leading to depletion of ATP and cell death, and has been used largely to understand dopaminergic neuronal death in Parkinson's disease (PD).[21] We used a concentration of MPP+ (3 mM) that produced a significant but moderate decrease (35%) in cell viability. MPP+ (3 mM) pro-

duced a stronger decrease in cell viability by the sncRNA-ASO used a positive control (70%), compared with basal, untreated conditions (60%) (Figure 2), and permitted the identification of other sncRNA-ASOs that worsen the response or protect it from MPP+ stress (Figure 1).

A total of 60 miRNA-ASOs impaired the effect of MPP+ in cell viability according to both statistical methods (Table 2), of which 22 (36.6%) were common to those that decrease cell viability under basal conditions (Table 1). A miEAA analysis with the group of miRNAs whose ASOs worsened the response to MPP+ stress pointed to response to *reactive oxygen species* (ROS) and *apoptosis* pathways (Table S4). In addition, 40 miRNA-ASOs protected from the detrimental effect of MPP+ on cell viability (Table 2).

In summary, the HTFS identified 85 miRNA-ASOs with a detrimental effect in basal conditions and/or in response to MPP+, and 40 miRNA-ASOs that protect from MPP+ stress, which may reflect the protective and detrimental roles of the targeted miRNAs, respectively.

A Subset of Detrimental miRNA-ASOs Increases Free Radical Biogenesis and Impairs Mitochondrial Function

Generation of ROS plays a critical role in damaging cellular components and initiating cell death. Therefore, we evaluated whether the effect of specific miRNA-ASOs in cell viability is linked to changes in ROS levels. We used CellROX Deep Red Reagent (Molecular Probes) to quantify ROS levels that were expressed with respect to the total number of cells, measured with CyQUANT Direct Cell Proliferation Assay (Invitrogen). This strategy permitted the detection of increased ROS levels in cells transfected with the miRNA-ASO used as a positive control, and a general increase in ROS levels in cells treated with 3 mM MPP+ (Figure S3).

We chose a subset of miRNA-ASOs with a negative effect on cell viability under basal conditions and/or in response to MPP+, a group of miRNA-ASOs that protect against MPP+, and a subset of miRNA-ASOs with no effect on cell viability. The subsets of detrimental and protective miRNA-ASOs are based on the altered expression of the targeted miRNAs in neurodegenerative conditions (Table S5). We particularly focused on miRNAs perturbed in PD paradigms, since differentiated SH-SY5Y cells are widely used to understand neuronal death mechanisms in this disease.[21] After transfection of the chosen miRNA-ASOs we evaluated ROS levels, both under basal conditions and in response to MPP+, as an alternative readout of cell dysfunction (Figure 3). We calculated Pearson's correlation coefficient to evaluate the degree of association between the cell viability (B score) and OS (ROS levels) measures. The statistically significant negative correlation coefficient (Figure S4) suggests that both measures are inversely associated.

Table 1. sncRNA-ASOs Decreasing Cell Viability

sncRNA ID	Replicate 1	Replicate 2	Replicate 3	Average
hsa-miR-1236-3p[a]	−15.43	−3.66	−5.84	−8.31
hsa-miR-4758-3p[a]	−8.84	−5.99	−9.63	−8.15
hsa-miR-1913[a]	−9.25	−8.26	−6.50	−8.00
hsa-miR-5006-3p[a]	−12.47	−5.29	−5.83	−7.86
hsa-miR-3677-5p[a]	−6.53	−5.42	−8.23	−6.73
hsa-miR-204-5p[a]	−4.99	−2.48	−12.39	−6.62
hsa-miR-4640-3p[a]	−4.56	−6.80	−8.14	−6.50
hsa-miR-496[a]	−3.48	−10.49	−4.55	−6.18
hsa-miR-5579-3p[a]	−6.94	−7.57	−3.89	−6.14
hsa-miR-6817-3p[a]	−5.11	−8.36	−4.89	−6.12
hsa-miR-3171[a]	−7.03	−6.81	−3.88	−5.91
hsa-miR-6840-5p[a]	−9.52	−4.47	−2.48	−5.49
hsa-miR-6511a-3p[a]	−3.70	−3.80	−8.34	−5.28
hsa-miR-2355-5p[a]	−1.80	−7.51	−6.33	−5.21
hsa-miR-1224-3p[a]	−2.68	−4.31	−8.14	−5.04
hsa-miR-24-1-5p[a]	−0.21	−7.64	−6.88	−4.91
hsa-miR-133a-3p[a]	−0.47	−4.26	−9.79	−4.84
hsa-miR-346[a]	−5.00	−4.97	−4.55	−4.84
hsa-miR-3940-3p[a]	−7.26	−2.62	−4.64	−4.84
hsa-miR-454-5p[a]	−1.55	−4.50	−8.32	−4.79
hsa-miR-7976[a]	−6.17	−3.79	−4.34	−4.77
hsa-miR-574-3p[a]	−2.62	−8.13	−3.47	−4.74
hsa-miR-361-3p[a]	−6.68	−2.09		−4.39
hsa-miR-5587-3p	−4.67	−4.73	−3.36	−4.25
hsa-miR-7-1-3p	−4.81	−3.13		−3.97
hsa-miR-3200-3p[a]	−3.05	−2.10	−6.76	−3.97
hsa-miR-374b-5p[a]	−3.00	−1.92	−6.93	−3.95
hsa-miR-6511b-3p	−3.38	−1.08	−7.11	−3.86
hsa-miR-4484[a]	−2.52	−4.60	−4.15	−3.76
hsa-miR-532-3p[a]	−4.42	−3.76	−2.60	−3.59
hsa-miR-3176	−3.30	−2.62	−4.85	−3.59
hsa-miR-6770-5p	−2.66	−3.98	−4.08	−3.57
hsa-miR-500a-3p[a]	−4.79	−2.52	−3.30	−3.54
hsa-miR-6800-3p[a]	−2.09	−4.44	−4.06	−3.53
hsa-miR-1301-3p	−4.18	−2.91	−3.31	−3.47
hsa-miR-2114-5p	−2.68	−8.04	0.37	−3.45
hsa-miR-4647	−2.13	−3.55	−4.60	−3.43
hsa-miR-4793-3p	−1.59	−4.78	−3.84	−3.40
hsa-miR-324-3p[a]	−1.33	−4.21	−4.11	−3.22
hsa-miR-767-3p[a]	−4.18	−3.75	−1.50	−3.14
hsa-miR-210-5p	−0.93	−2.28	−6.08	−3.10
hsa-miR-1914-5p[a]	−3.14	−5.55	−0.59	−3.09
hsa-miR-6738-3p[a]	−2.40	−3.90	−2.93	−3.08
hsa-miR-551b-3p[a]	−1.95	−1.64	−5.46	−3.02

(Continued)

Table 1. Continued

sncRNA ID	Replicate 1	Replicate 2	Replicate 3	Average
hsa-miR-18a-5p[a]	−2.70	−3.34	−2.97	−3.00
hsa-miR-152-5p	−3.01	−3.25	−2.70	−2.99
hsa-miR-766-3p[a]	−2.37	−0.80	−5.65	−2.94
hsa-miR-5699-5p	−5.14	−1.55	−2.12	−2.94
hsa-miR-767-5p	−2.19	−4.43	−2.16	−2.93
hsa-miR-7974[a]	−2.35	−4.66	−1.67	−2.89
hsa-miR-642a-5p	−1.15	−4.95	−2.58	−2.89
hsa-miR-362-5p	−2.97	−3.39	−2.27	−2.88
hsa-miR-3116	−3.25	−3.10	−2.25	−2.87
hsa-miR-885-5p[a]	−2.43	−4.03	−2.05	−2.84
hsa-miR-2116-3p[a]	−4.35	−0.76	−3.39	−2.83
hsa-miR-636	−2.76	−1.39	−3.96	−2.70
hsa-miR-330-3p	−2.97	−3.20	−1.90	−2.69
hsa-miR-6803-3p	−1.00	−2.87	−4.02	−2.63
hsa-miR-106b-3p	−2.02	−0.75	−5.09	−2.62
hsa-miR-543[a]	−2.08	−3.87	−1.90	−2.62
hsa-miR-654-3p[a]	−0.64	−2.40	−4.79	−2.61
hsa-miR-151a-5p	−1.96	−2.18	−3.45	−2.53
hsa-miR-4685-3p[a]	−0.08	−3.24	−4.19	−2.50
hsa-miR-1298-5p	−1.66	−2.84	−2.68	−2.39
hsa-miR-1234-3p[a]	−3.30	−2.10	−1.75	−2.38
hsa-miR-758-5p	−2.70	−2.76	−1.68	−2.38
hsa-miR-4638-3p	−1.39	−2.76	−2.92	−2.35
hsa-miR-2355-3p	−2.18	−0.90	−3.94	−2.34
hsa-miR-939-3p[a]	−3.70	−2.86	−0.45	−2.34
hsa-miR-1305	−1.72	−2.12	−3.02	−2.29
hsa-miR-616-5p[a]	−2.53	−2.84	−1.45	−2.27
hsa-miR-590-3p	−0.10	−3.63	−3.05	−2.26
hsa-miR-3130-5p[a]	−2.49	0.02	−4.17	−2.22
hsa-miR-551a	−2.56	−3.79	−0.11	−2.15
hsa-miR-128-3p	−3.24	−1.99	−1.19	−2.14
hsa-miR-3944-3p	−2.39	−0.45	−3.27	−2.03

Hits show a median polished B score < −2, consistent in at least two biological replicates. Only ASOs targeting sncRNAs with mean normalized counts >1 in differentiated SHSY5Y cells are shown.
[a]Hits validated with a LMM.

miRNA-ASOs impairing cell viability induced a significant increase in ROS levels under basal conditions and in response to MPP+ (Exp 1; Figure 3C). The miRNAs-ASOs impairing cell viability, in both basal conditions and response to OS, strongly contributed to increased ROS levels (Exp 2a versus Exp 2b, upper panel; Figure 3C). miRNA-ASOs with no effect on cell viability induced a slight increase in ROS levels compared with mock-transfected cells, suggesting that LNA-ASOs may produce minor OS (Exp 4; Figure 3C). Compared with this group, protective miRNA-ASOs tended to decrease ROS levels (Exp 3; Figure 3C) in agreement with their protective outcome

Table 2. sncRNA-ASOs That Modify the Cell Response to Oxidative Stress

sncRNA-ASO	Replicate 1	Replicate 2	Replicate 3	Average	sncRNA-ASO	Replicate 1	Replicate 2	Replicate 3	Average
hsa-miR-636[a]	−11.08	−8.06	−7.50	−8.88	hsa-miR-363-5p	−1.93	−3.91	−0.97	−2.27
hsa-miR-6840-5p[a]	**-7.63**	**-8.46**	**-5.76**	**-7.28**	hsa-miR-146b-3p[a]	−2.60	−2.69	−1.52	−2.27
hsa-miR-204-5p[a]	**-6.19**	**-7.23**	**-7.66**	**-7.03**	hsa-miR-410-3p[a]	−2.42	−2.92	−1.46	−2.27
hsa-miR-1236-3p[a]	**-8.41**	**-7.02**	**-4.92**	**-6.78**	hsa-miR-330-3p	−2.34	−2.43	−2.02	−2.26
hsa-miR-532-3p[a]	**-8.45**	**-5.70**	**-5.86**	**-6.67**	hsa-miR-1253	−3.69	−2.01	−1.07	−2.26
hsa-miR-5006-3p[a]	**-4.23**	**-8.42**	**-5.45**	**-6.03**	hsa-miR-6806-3p	−2.13	−3.79	−0.84	−2.25
hsa-miR-6803-3p	−9.90	−3.96	−3.26	−5.71	hsa-miR-6857-3p	−2.14	−3.98	−0.50	−2.21
hsa-miR-6817-3p[a]	**-3.66**	**-4.75**	**-7.49**	**-5.30**	**hsa-miR-574-3p[a]**	**-2.55**	**-1.41**	**-2.66**	**-2.21**
hsa-miR-362-5p[a]	−4.45	−4.87	−6.14	−5.16	**hsa-miR-6511a-3p[a]**	**-2.67**	**-2.14**	**-1.80**	**-2.20**
hsa-miR-1271-5p[a]	−2.38	−4.76	−8.01	−5.05	hsa-miR-129-2-3p[a]	−1.54	−2.32	−2.74	−2.20
hsa-miR-2355-5p[a]	**-3.03**	**-6.88**	**-4.29**	**-4.74**	hsa-miR-3176[a]	−2.60	−2.87	−1.10	−2.19
hsa-miR-4522	−4.50	−6.35	−3.15	−4.67	hsa-miR-99b-5p	−2.89	−1.49	−2.15	−2.18
hsa-miR-1913[a]	**-5.73**	**-2.95**	**-5.31**	**-4.66**	hsa-miR-6797-3p[a]	−2.62	−2.89	−0.81	−2.11
hsa-miR-454-5p[a]	**-7.71**	**-3.05**	**-3.00**	**-4.59**	hsa-miR-342-3p	−2.68	−0.59	−2.95	−2.07
hsa-miR-6511b-3p[a]	−5.59	−3.85	−4.26	−4.57	hsa-miR-548s	−2.83	−1.01	−2.33	−2.06
hsa-miR-4479	−3.90	−4.18	−5.39	−4.49	hsa-miR-4767[a]	−2.08	−2.71	−1.36	−2.05
hsa-miR-7977[a]	−6.04	−4.55	−2.62	−4.40	hsa-miR-615-3p	−2.25	−3.29	−0.55	−2.03
hsa-miR-133a-3p[a]	**-3.20**	**-5.02**	**-4.84**	**-4.35**	hsa-miR-143-5p	−3.48	−2.65	0.08	−2.01
hsa-miR-654-5p	−6.43	−3.00	−3.23	−4.22	hsa-miR-182-5p	−2.73	−2.37	0.61	−1.50
hsa-miR-767-5p[a]	−2.02	−4.82	−5.80	−4.21	hsa-miR-548b-5p[a]	−0.83	3.30	3.57	2.01
hsa-miR-24-2-5p[a]	−4.44	−2.25	−5.86	−4.18	hsa-miR-7854-3p[a]	0.41	2.89	2.89	2.06
hsa-miR-6750-3p	−5.93	−4.33	−1.98	−4.08	hsa-miR-4745-5p[a]	1.15	2.56	2.49	2.07
hsa-miR-615-5p[a]	−2.41	−4.51	−5.31	−4.07	hsa-miR-197-5p[a]	2.19	2.79	1.37	2.12
hsa-miR-642a-5p[a]	−1.02	−4.78	−6.32	−4.04	hsa-miR-6129[a]	2.01	3.18	1.19	2.12
hsa-miR-766-3p[a]	**-4.95**	**-3.95**	**-2.80**	**-3.90**	hsa-miR-548l	4.41	−0.52	2.77	2.22
hsa-miR-4685-3p[a]	**-2.77**	**-4.40**	**-4.32**	**-3.83**	hsa-miR-548b-3p	2.54	2.15	2.11	2.27
hsa-miR-346[a]	**-4.33**	**-3.04**		**-3.69**	hsa-miR-3126-5p[a]	0.26	4.11	2.65	2.34
hsa-miR-6798-3p[a]	−3.26	−3.42	−4.11	−3.59	hsa-miR-101-3p[a]	0.57	2.34	4.15	2.35
hsa-miR-4642[a]	−7.34	−3.31	−0.06	−3.57	hsa-miR-656-3p	0.95	2.94	3.26	2.38
hsa-miR-3619-5p	−4.64	−3.02	−2.95	−3.54	hsa-miR-4443[a]	1.04	2.03	4.10	2.39
hsa-miR-605-5p[a]	−3.41	−4.68	−2.50	−3.53	hsa-miR-5695[a]	3.73	1.95	1.82	2.50
hsa-miR-1226-5p	−3.29	−1.28	−5.77	−3.44	hsa-miR-505-5p[a]	5.36	−0.81	3.05	2.53
hsa-miR-4758-3p[a]	**-3.91**	**-1.23**	**-5.18**	**-3.44**	hsa-miR-9-3p	3.59	2.62	1.54	2.58
hsa-miR-1914-5p	−3.48	−2.52	−4.32	−3.44	hsa-miR-548k[a]	3.22	2.72	1.97	2.64
hsa-miR-5587-3p	**-2.10**	**-3.78**	**-4.38**	**-3.42**	hsa-miR-651-5p[a]	3.25	2.50	2.21	2.65
hsa-miR-152-5p	−6.01	−1.46	−2.69	−3.39	hsa-miR-876-5p[a]	0.00	5.17	2.97	2.71
hsa-miR-4800-3p	−5.11	−2.29	−2.63	−3.34	hsa-miR-425-3p	1.94	4.33	1.87	2.71
hsa-miR-339-5p[a]	−3.82	−2.36	−3.78	−3.32	hsa-miR-574-5p[a]	2.79	2.94	2.71	2.81
hsa-miR-767-3p[a]	**-2.00**	**-5.01**	**-2.93**	**-3.31**	hsa-miR-548e-3p[a]	5.30	2.28	0.94	2.84
hsa-miR-3938	−3.73	−3.39	−2.79	−3.30	hsa-miR-200c-3p[a]	1.36	3.20	3.98	2.85
hsa-miR-99a-5p[a]	−4.30	−2.27		−3.28	hsa-miR-629-5p[a]	2.70	1.49	4.48	2.89
hsa-miR-455-3p[a]	−3.94	−3.50	−2.38	−3.27	hsa-miR-766-5p	4.21	3.50	1.26	2.99
hsa-miR-26a-1-3p[a]	−4.39	−3.52	−1.74	−3.22	hsa-miR-1303[a]	0.67	4.57	3.76	3.00

(Continued on next page)

Table 2. Continued

sncRNA-ASO	Replicate 1	Replicate 2	Replicate 3	Average	sncRNA-ASO	Replicate 1	Replicate 2	Replicate 3	Average
hsa-miR-6738-3p[a]	**-3.19**	**-3.97**	**-2.47**	**-3.21**	hsa-miR-3163[a]	2.23	6.21	0.74	3.06
hsa-miR-874-5p[a]	−4.32	−1.80	−3.34	−3.16	hsa-miR-105-3p	1.44	3.84	3.91	3.07
hsa-miR-331-3p[a]	−2.94	−3.32		−3.13	hsa-miR-10b-3p[a]	5.86	0.92	2.67	3.15
hsa-miR-2277-3p	−2.64	−2.68	−4.00	−3.11	hsa-miR-215-5p[a]	3.49	2.96		3.23
hsa-miR-152-3p[a]	−2.32	−3.73		−3.03	hsa-miR-1185-5p[a]	3.30	1.95	4.92	3.39
hsa-miR-361-3p[a]	**-1.00**	**-4.74**	**-3.33**	**-3.03**	hsa-miR-3141[a]	0.14	2.70	7.48	3.44
hsa-miR-329-3p[a]	−3.24	−2.43	−3.40	−3.02	hsa-miR-1268a[a]	0.94	5.76	3.64	3.45
hsa-miR-4516	−3.59	−3.68	−1.68	−2.98	hsa-miR-193b-5p[a]	1.48	3.86	5.04	3.46
hsa-miR-3130-5p	−5.37	−3.71	0.15	−2.98	hsa-miR-4705[a]	3.57	4.43	2.41	3.47
hsa-miR-370-5p	−2.46	−3.19	−3.21	−2.96	hsa-miR-3609[a]	2.18	2.82	6.28	3.76
hsa-miR-6800-3p[a]	**-4.01**	**-2.06**	**-2.79**	**-2.95**	hsa-miR-320[a]	4.71	2.91		3.81
hsa-miR-105-5p[a]	−4.71	−3.74	−0.28	−2.91	hsa-miR-221-5p[a]	6.00	1.98	3.52	3.83
hsa-miR-106b-3p	−1.71	−3.65	−3.30	−2.89	hsa-miR-219a-1-3p[a]	6.93	3.64	1.00	3.86
hsa-miR-6726-3p[a]	−4.97	−2.07	−1.49	−2.84	hsa-miR-29b-1-5p[a]	2.71	4.73	4.21	3.88
hsa-miR-4746-5p[a]	−2.24	−3.82	−2.35	−2.80	hsa-miR-1277-3p[a]	5.78	3.07	3.06	3.97
hsa-miR-151a-5p	−2.58	−2.88	−2.86	−2.77	hsa-miR-134-5p[a]	3.63	4.96	3.34	3.98
hsa-miR-15a-3p	−3.22	−3.81	−1.16	−2.73	hsa-miR-1269p[a]	6.33	3.70	1.99	4.01
hsa-miR-3187-3p[a]	−3.30	−1.91	−2.84	−2.69	hsa-miR-627-5p	1.43	7.54	3.40	4.12
hsa-miR-129-1-3p[a]	0.67	−3.15	−5.52	−2.67	hsa-miR-590-5p	5.24	3.92	3.44	4.20
hsa-miR-496[a]	**-2.42**	**-1.26**	**-4.29**	**-2.65**	hsa-miR-99a-3p[a]	6.49	2.23	4.41	4.38
hsa-miR-23a-3p[a]	−4.22	−2.13	−1.55	−2.63	hsa-miR-147p[a]	5.29	4.50	4.11	4.63
hsa-miR-1296-3p[a]	−0.81	−2.87	−4.11	−2.60	hsa-miR-585-3p[a]	3.89	5.75	4.51	4.72
hsa-miR-1538	−3.61	−2.28	−1.79	−2.56	hsa-miR-186-3p[a]	5.11	4.76	4.29	4.72
hsa-miR-148a-5p[a]	−1.35	−3.27	−2.78	−2.47	hsa-miR-664a-5p[a]	7.02	2.83	4.92	4.92
hsa-miR-550a-3p[a]	−4.37	−0.79	−2.14	−2.43	hsa-miR-6847-5p[a]	7.62	3.90	3.65	5.06
hsa-let-7d-3p[a]	−1.21	−3.76	−2.12	−2.36	hsa-miR-1268b[a]	12.43	9.03	7.61	9.69

Hits show a median polished B score <−2; worsening cell viability in response to MPP[+]; or B score >2, which protects against the detrimental effect of MPP[+], consistent between at least two biological replicates. Only ASOs targeting sncRNAs with mean normalized counts >1 in differentiated SHSY5Y cells treated with 3 mM MPP[+] for 24 h, are shown. ASOs highlighted in bold are common to those found in basal conditions (Table 1).
[a]Hits validated with a LMM.

in viability determinations. Overall, these data indicate that ROS levels confirm the previously selected hits, especially those producing a detrimental effect on cell viability.

To test whether the detrimental effect of miRNA-ASOs was linked to mitochondrial dysfunction, we measured the mitochondrial membrane potential by using Mitotracker fluorescent dye (Molecular Probes). We selected ASOs targeting miR-204-5p, miR-532-3p, and miR-324-3p, which are reliably expressed in the human brain, perturbed in several neurodegenerative and neurological disorders,[20,25–31] and involved in neuronal differentiation.[32–34]
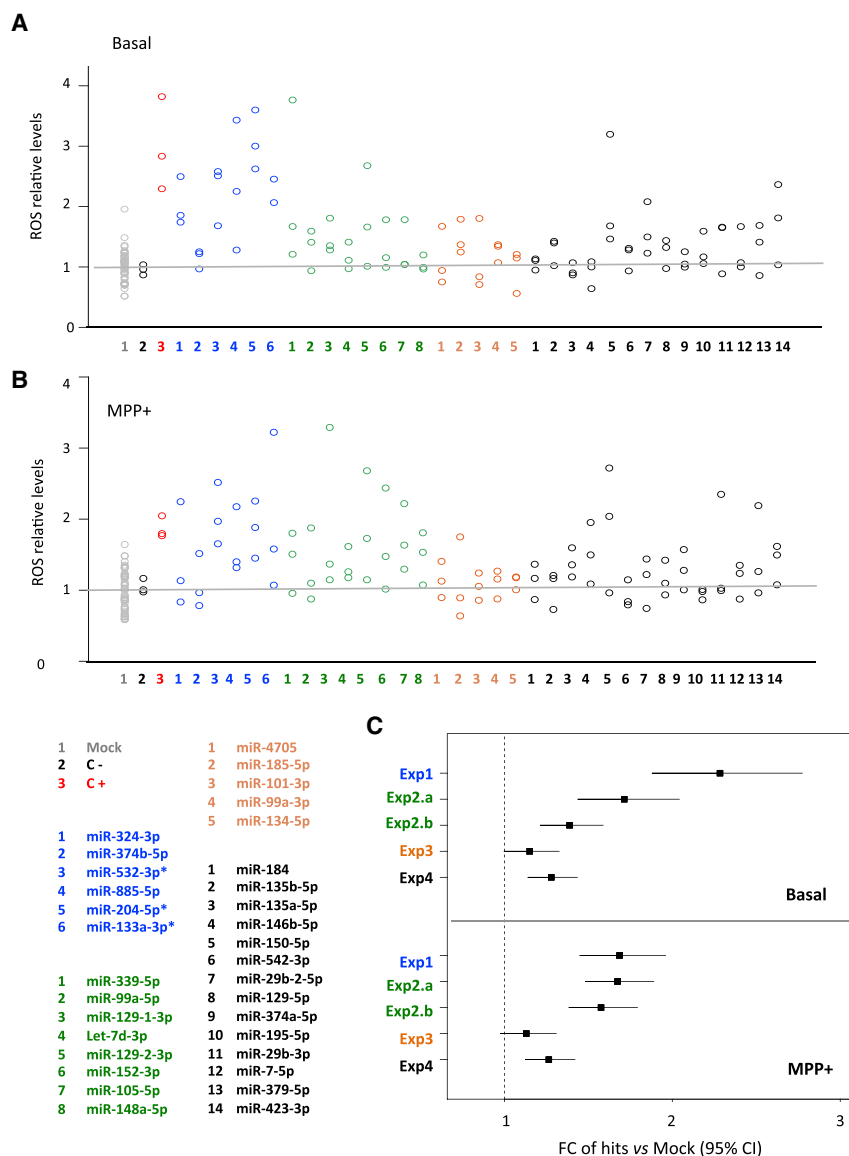
Confirming the effect of three miRNA-ASOs in decreasing cell viability (Tables 1 and 2) and inducing ROS, miR-204-5p-, miR-324-3p-, and miR-532-3p-ASO significantly impaired mitochondrial membrane potential (Figure 4). These results suggest that

the activity of these miRNAs is important for neuronal survival and response to MPP+ stress.

miRNA Expression Dynamics in Response to MPP+ May Contribute to Cell Dysfunction

Inhibition of sncRNAs activity may reflect, at least to some extent, the consequences of the downregulation of the targeted sncRNAs that occurs in response to specific stimuli. We analyzed the sncRNA expression profiles in response to MPP+ to understand if sncRNA dynamics contribute to cell viability outcome. SH-SY5Y cells were differentiated, and sncRNA expression profiles were determined by deep sequencing 24 h after exposure to MPP+ (3 mM). A total of 128 miRNAs were significantly deregulated after exposure to MPP+ (Table 3).

Among the miRNAs whose ASOs worsened cell viability in basal conditions and/or response to MPP+ (according to both statistical tests),

A Basal

B MPP+

C

1	Mock	1	miR-4705
2	C -	2	miR-185-5p
3	C +	3	miR-101-3p
		4	miR-99a-3p
		5	miR-134-5p
1	miR-324-3p		
2	miR-374b-5p	1	miR-184
3	miR-532-3p*	2	miR-135b-5p
4	miR-885-5p	3	miR-135a-5p
5	miR-204-5p*	4	miR-146b-5p
6	miR-133a-3p*	5	miR-150-5p
		6	miR-542-3p
1	miR-339-5p	7	miR-29b-2-5p
2	miR-99a-5p	8	miR-129-5p
3	miR-129-1-3p	9	miR-374a-5p
4	Let-7d-3p	10	miR-195-5p
5	miR-129-2-3p	11	miR-29b-3p
6	miR-152-3p	12	miR-7-5p
7	miR-105-5p	13	miR-379-5p
8	miR-148a-5p	14	miR-423-3p

Figure 3. Validation of HTFS Hits Based on the Evaluation of ROS Levels

Plots of relative ROS levels in cells transfected with sncRNA-ASOs in basal conditions (A) and after exposure to 3 mM MPP+ (B). ROS levels in each biological replicate are represented by a dot and expressed relative to a control mock-transfected well. In the plots, numbers, and colors correspond to the diverse transfected sncRNA-ASOs: blue, sncRNA-ASOs that impair cell viability in basal conditions (asterisks label miRNA-ASOs that impair cell viability both under basal conditions and in response to MPP+); green, sncRNA-ASOs that worsen cell viability in response to MPP+; orange, sncRNA-ASOs that protect against MPP+; black, ncRNA-ASOs with no effect on cell viability, including a scrambled sequence used as a negative control (C−); red, an ASO with a known toxic effect used as a positive control (C+). (C) Plot showing the fold change (FC) of ROS levels in cells transfected with miRNA-ASOs versus mock-transfected cells, under basal conditions (upper panel) or in response to MPP+ (lower panel). Exp1: FC considering the miRNA-ASOs in blue; Exp2a, FC considering miRNA-ASOs in green and those in blue marked with an asterisk; Exp2b, FC considering miRNA-ASOs in green; Exp3, FC considering miRNA-ASOs in orange; and Exp4, FC considering miRNA-ASOs in black.

oxidative stress response, *p53*, and *DNA damage response*. In addition, MPP+-upregulated miRNAs were enriched in analogous pathways. Furthermore, MPP+-deregulated miRNAs were significantly perturbed in Alzheimer's-, Parkinson's-, and Huntington's-disease-related pathways. Overall, these data suggest that the miRNA expression dynamics in response to MPP+ contributes to detrimental processes.

DISCUSSION

The evidence shows that perturbed activity of specific sncRNAs influence neuronal function under both normal and pathological conditions. In the present study we developed an HTFS to generally identify sncRNAs involved in neuronal cell viability, both under basal conditions and in response to OS, a major player in neurodegenerative processes.

Here, we used LNA-modified AOs that bind to target sequences and decrease the availability and activity of each particular sncRNA. Although LNA modifications in ASOs increase stability and specificity for the target sequence,[35] binding to unintended targets could account for nonspecific effects in cell viability. However, the significant enrichment of hits among SH-SY5Y-expressed sncRNAs favors the idea that LNA-ASOs induce a detrimental effect by specifically targeting sncRNAs expressed in our model system.

To identify reliable sncRNA-ASOs affecting cell viability, we used the B score method, which is designed to detect hits in HTFS.[19] We

hsa-miR-7974, miR-3619-5p, miR-455-3p, miR-3176, miR-3187-3p, miR-636, and miR-454-5p were downregulated after exposure to MPP+ (Table 3), which suggests that their deregulation pattern may contribute to impairment of cell viability. For four downregulated miRNAs—miR-4745-5p, miR-574-5p, miR-1303, and miR-6847-5p—the correspondent ASOs protected from MPP+ stress. Among the MPP+-downregulated miRNAs, the increased number of detrimental ASOs versus protective ones is in contrast with the few hits found among the MPP+-upregulated miRNAs (only one protective and one detrimental miRNA-ASO).

We used the miEAA tool to identify the pathways targeted by MPP+-deregulated miRNAs (Tables S6 and S7). The analysis showed that MPP+-downregulated miRNAs were significantly depleted in signaling pathways related to stress, including *apoptosis*,
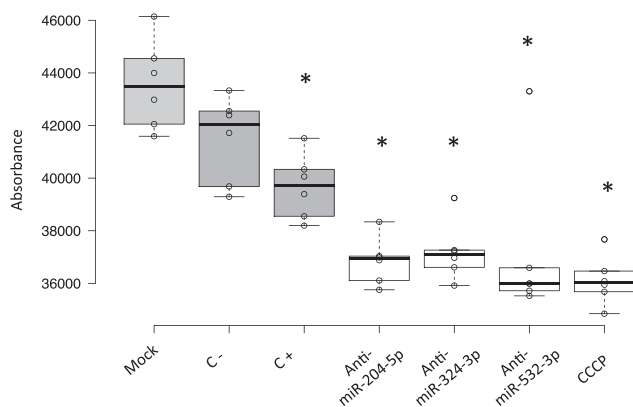
Figure 4. Mitochondrial Activity after Transfection with Specific miRNA-ASOs

Mock, cells treated with Lipofectamine; negative control (C−), cells transfected with an ASO that does not produce any effect in cell viability; positive control (C+), cells transfected with a control sncRNA-ASO inducing cell death; positive control (CCCP), cells treated with CCCP were used as a positive control for mitochondrial functional loss. The boxplot shows absorbance determinations after incubation with MitoTracker Deep Red reagent. *p < 0.001, by the Kruskal-Wallis test, followed by the Mann-Whitney U test with Bonferroni's correction as a post hoc test (n = 5).

applied an iterative median polish that robustly avoids row- and column-position-related systematic errors, which we detected in the different HTFSs. Z scores are also based on the raw sample values; however, as Brideau and colleagues[19] discussed, these scores suffer from the fact that they do not take into account positional effects, and their performance is compromised by outliers, which are the key hits. However, when no positional effects and changes occur in a plate, Z scores are slightly more efficient. That is why the combination of different methods may help to choose the best top hits. Under this premise, we proposed another statistical approach that is based on Z scores, but improved in a way similar to the B score. The approach is based on a LMM, where the positional effects are taken into account, and, in addition, it considers the three independent replicates as a source of variability in the experimental design. This method detected from 55% to 70% of the B score hits, and additional functional validations were performed for a subset of sncRNA-ASOs commonly identified in both strategies.

Only sncRNA-ASOs targeting canonical miRNAs produced significant effects in cell viability in agreement with both statistical methods. According to the miEAA (Tables S3 and S4), the pathways targeted by the group of miRNAs whose ASOs decrease cell viability favor the idea that the detrimental effects of the miRNA-ASOs are not nonspecific but are caused by the selective blockage of miRNAs that participate in neuronal survival.

miRNA-ASOs that impair cell viability in basal conditions and/or in response to MPP+ may prevent the activity of miRNAs involved in neuronal maintenance or in neuronal protection in front of OS. Conversely, miRNA-ASOs protecting from MPP+ stress may target miRNAs contributing to MPP+-mediated cell death. Our results

have validated the toxic effect of miRNA-ASOs tested in other HTFSs, including miR-204; miR-210 inhibitors in HeLa cells;[36] and miR-133a-3p, miR-361-3p, and miR-346 inhibitors in lung cancer cells.[37] In addition, in line with the detrimental effect of the miR-7-1-3p-ASO observed in the present study, miR-7-1 activity is involved in motor neuron protection.[38] miR-134-5p expression induces neuronal death in the brain,[39] which agrees with the protective effect of miR-134-5p-ASO in front of the stressful conditions observed here. Furthermore, reduction of miR-23a following traumatic brain injury induces neuronal death,[40] which matches with the worsened effect of the correspondent ASO observed in the present study.

Although our results validate many of the miRNAs reported to have a role in cell viability, there are some exceptions. The present study did not reveal the neuroprotective activity of miR-7-5p and miR-153.[41] In addition, we did not reproduce the neuroprotective effect of miR-181 inhibition[42] or the detrimental effect of miR-29b inhibition[43] in front of cerebral ischemia. Whether the lack of confirmation is because the activity of these miRNAs is context dependent or involves alternative experimental conditions remains to be determined. Validation of the present results in diverse cell types, including primary neurons, is needed to understand how general and consistent the effects of the miRNA-ASOs reported herein are. Furthermore, evaluation of the effect of miRNA-ASOs in the brain in model organisms will answer whether validation in simpler neuronal cell cultures can be extended to a complex structure with heterogeneous neuronal and non-neuronal (glial) cells.

The temporal and spatial miRNA dynamics regulate gene expression programs in normal conditions and in response to stressful stimuli. The effect of miRNA-ASOs mimic the consequences of miRNA downregulation, and our data suggest that the overall miRNA expression patterns in response to MPP+ contribute to MPP+-mediated damage. Analogous assumptions considering the miRNA expression patterns in human brains in neurodegenerative conditions are difficult to determine. Neurodegenerative diseases involve continuous and long-lasting molecular changes that shape disease evolution. For instance, according to our data, miR-204-5p and miR-532-3p are protective miRNAs (their inhibition impairs cell viability). In the *substantia nigra* of PD patients, miR-204-5p is upregulated, and miR-532-5p is downregulated;[27] however, both miRNAs are downregulated in the *amygdala* of PD patients.[20,27] It is difficult to anticipate the significance of these changes, since neuropathological alterations strongly differ in these two brain areas. Furthermore, the expression pattern of miR-128-3p, another miRNA that we have identified as neuroprotective, differs in the *amygdala* of PD patients, showing downregulation at pre-clinical stages and upregulation at clinical stages.[20] miRNA expression dynamics may reflect complex reactive responses with functional consequences, either protecting from stress or contributing to dysfunction, depending on the brain regions and disease evolutionary stages. Experimentally induced alterations in the activity of miRNAs *in vivo* should highlight the relevance that changes in the expression levels of particular miRNA (or groups of miRNAs) undergo in a pathogenic process.

Table 3. miRNAs Significantly Deregulated, 24 h after Treatment with 3 mM MPP

miRNA	Mean Normalized Counts	Log$_2$ Fold Change 24 h MPP$^+$ versus C	p$_{adj}$	Average B Score Basal Assay	Average B Score MPP$^+$ Assay	miRNA	Mean Normalized Counts	Log^2 Fold Change 24 h MPP$^+$ versus C	p$_{adj}$	Average B Score Basal Assay	Average B Score MPP$^+$ Assay
hsa-let-7a-5p	212,828.53	−0.46	0.01	3.00	0.77	hsa-miR-335-5p	33.84	−0.73	0.02	1.29	−0.30
hsa-let-7c-5p	9,910.12	−0.47	0.03	0.65	1.51	hsa-miR-34a-3p	65.64	1.09	0.00	−1.18	−1.46
hsa-let-7f-1-3p	37.86	−1.00	0.00	0.48	−0.09	hsa-miR-34a-5p	1,366.74	0.98	0.00	−1.50	−0.58
hsa-let-7i-5p	23,119.45	0.34	0.00	−1.18	−0.45	hsa-miR-34b-3p	17.96	1.54	0.00	0.27	−0.06
hsa-miR-10a-5p	628.77	−0.53	0.04	3.57	−0.95	hsa-miR-34b-5p	62.77	1.88	0.00	1.16	−1.58
hsa-miR-1180-3p	1,366.77	−0.60	0.00	1.57	1.06	hsa-miR-34c-5p	1,062.35	1.91	0.00	−0.60	0.81
hsa-miR-1224-5p	83.98	0.60	0.01	1.72	0.90	hsa-miR-3615	1,227.71	−0.40	0.02	−0.02	−0.14
hsa-miR-1247-5p	78.77	0.60	0.00	−1.73	−1.92	hsa-miR-3619-5p	15.30	−1.73	0.00	0.54	−3.54
hsa-miR-125b-1-3p	1,030.31	−0.47	0.01	2.16	−0.35	hsa-miR-3679-5p	20.00	−0.97	0.01	0.44	−0.70
hsa-miR-126-3p	1,021.38	0.21	0.03	0.28	−0.92	hsa-miR-378a-3p	3,805.50	0.41	0.00	−0.30	1.17
hsa-miR-126-5p	5,597.90	0.39	0.00	0.94	−0.01	hsa-miR-378i	14.00	0.92	0.01	1.29	−1.45
hsa-miR-1260a	3,628.71	0.81	0.00	3.77	−0.74	hsa-miR-381-3p	1,565.58	0.36	0.00	−0.45	−1.67
hsa-miR-1260b	3,920.23	0.79	0.00	−1.47	−0.33	hsa-miR-3909	142.17	0.62	0.00	−2.21	−0.58
hsa-miR-1272	13.23	−2.00	0.00	0.95	−0.97	hsa-miR-3929	44.66	1.10	0.00	0.80	−1.60
hsa-miR-1276	240.10	−0.56	0.00	−1.67	−1.00	hsa-miR-3939	17.64	−0.78	0.02	0.08	−1.33
hsa-miR-1298-3p	14.61	1.45	0.00	1.30	0.26	hsa-miR-409-3p	1,080.93	−0.36	0.01	−1.63	−1.60
hsa-miR-1298-5p	289.63	1.68	0.00	−2.39	−1.76	hsa-miR-424-5p	312.73	0.64	0.00	0.13	0.04
hsa-miR-1303	152.76	−1.30	0.00	0.89	3.00	hsa-miR-425-3p	924.49	0.33	0.00	0.15	2.71
hsa-miR-130b-5p	2,949.55	−0.41	0.00	−0.75	−0.19	hsa-miR-4284	28.38	2.82	0.00	−0.41	−0.42
hsa-miR-132-3p	6,025.80	−0.67	0.02	1.22	0.25	hsa-miR-4301	53.24	1.15	0.00	1.34	−0.50
hsa-miR-135a-3p	73.40	−0.88	0.00	−0.77	0.25	hsa-miR-4455	455.18	−0.90	0.00	2.71	1.17
hsa-miR-135a-5p	143.13	−0.51	0.03	0.15	1.36	hsa-miR-448	79.61	1.00	0.00	0.24	2.77
hsa-miR-138-1-3p	547.79	−0.86	0.00	−2.14	−0.95	hsa-miR-449a	47.36	0.57	0.03	−0.42	0.47
hsa-miR-140-3p	7,556.14	0.25	0.02	−0.13	−1.61	hsa-miR-4516	15.07	0.96	0.01	−0.41	−2.98
hsa-miR-146a-5p	77.95	0.51	0.04	−1.97	−0.42	hsa-miR-454-5p	459.79	−0.42	0.01	−4.79	−4.59
hsa-miR-149-5p	3,328.89	0.49	0.00	−1.38	−0.60	hsa-miR-455-3p	65.94	−0.80	0.03	0.20	−3.27
hsa-miR-152-5p	367.41	0.29	0.03	3.41	−3.39	hsa-miR-4638-3p	24.56	−0.70	0.04	−2.35	−1.40
hsa-miR-17-5p	13,154.08	−0.22	0.01	1.15	−1.85	hsa-miR-4741	79.93	−0.72	0.01	−0.24	−0.13
hsa-miR-181a-3p	1,831.47	0.50	0.00	0.30	−0.37	hsa-miR-4745-5p	60.91	−0.79	0.03	0.80	2.07
hsa-miR-182-5p	46,002.45	0.39	0.04	0.03	−1.50	hsa-miR-4792	680.59	1.29	0.00	−0.58	−1.29
hsa-miR-183-3p	148.31	0.62	0.00	−0.10	−1.35	hsa-miR-483-3p	69.91	1.22	0.00	−0.56	−2.00
hsa-miR-183-5p	5,824.28	0.38	0.01	−0.46	−0.42	hsa-miR-486-3p	81.75	0.82	0.03	−0.34	−0.38
hsa-miR-1908-5p	48.76	−0.72	0.01	2.47	1.93	hsa-miR-486-5p	5,471.97	0.55	0.01	1.76	−1.36
hsa-miR-192-5p	5,963.58	0.79	0.00	−0.19	0.55	hsa-miR-489-3p	709.95	1.86	0.00	−0.33	−1.31
hsa-miR-193a-5p	62.50	−0.75	0.02	−1.44	1.57	hsa-miR-490-5p	37.79	−0.99	0.00	0.28	0.37
hsa-miR-193b-3p	235.11	−0.32	0.04	0.43	−1.42	hsa-miR-497-5p	2,210.67	0.40	0.04	4.12	0.67
hsa-miR-194-5p	429.58	0.49	0.00	0.15	0.24	hsa-miR-499a-5p	25.96	1.20	0.00	0.30	1.77
hsa-miR-195-3p	154.61	0.54	0.00	−1.92	−1.10	hsa-miR-501-3p	5,352.55	−0.38	0.04	−0.56	0.45
hsa-miR-195-5p	1,398.68	0.55	0.01	−1.09	−0.51	hsa-miR-532-5p	12,026.27	0.23	0.05	0.08	−1.33
hsa-miR-197-3p	4,746.12	0.47	0.00	−1.20	−1.18	hsa-miR-548h-5p	53.59	0.52	0.03	2.32	0.54
hsa-miR-200b-3p	20.49	0.64	0.03	0.36	−0.71	hsa-miR-550a-3p	258.48	0.42	0.01	0.10	−2.43
hsa-miR-20b-5p	584.11	−0.50	0.00	0.95	1.24	hsa-miR-550a-5p	316.40	0.45	0.00	1.19	1.03

(Continued on next page)

Table 3. Continued

miRNA	Mean Normalized Counts	Log$_2$ Fold Change 24 h MPP$^+$ versus C	p$_{adj}$	Average B Score Basal Assay	Average B Score MPP$^+$ Assay	miRNA	Mean Normalized Counts	Log^2 Fold Change 24 h MPP$^+$ versus C	p$_{adj}$	Average B Score Basal Assay	Average B Score MPP$^+$ Assay
hsa-miR-210-5p	73.28	−0.46	0.04	−3.10	0.42	hsa-miR-574-5p	752.87	−0.90	0.00	1.27	2.81
hsa-miR-212-3p	1,057.58	−0.77	0.02	1.72	−0.09	hsa-miR-576-5p	202.17	0.51	0.00	1.29	1.47
hsa-miR-212-5p	423.95	−0.75	0.01	1.03	0.47	hsa-miR-584-5p	1,617.69	0.62	0.00	−0.25	1.63
hsa-miR-219a-1-3p	35.29	0.54	0.03	0.02	3.86	hsa-miR-627-5p	70.33	0.78	0.00	1.48	4.12
hsa-miR-22-3p	183,682.84	0.16	0.03	−0.15	0.09	hsa-miR-636	57.03	−0.82	0.00	−2.70	−8.88
hsa-miR-222-3p	734.01	−0.32	0.02	0.24	0.67	hsa-miR-6516-5p	27.95	−0.72	0.01	1.00	−0.41
hsa-miR-23a-5p	126.01	−0.89	0.00	0.62	−0.30	hsa-miR-653-3p	60.24	1.85	0.00	1.38	2.09
hsa-miR-25-5p	984.00	−0.51	0.00	0.60	−0.70	hsa-miR-653-5p	60.58	1.39	0.00	2.44	−0.06
hsa-miR-26b-3p	273.41	−0.38	0.04	−2.73	1.31	hsa-miR-671-3p	2,130.38	0.44	0.02	0.00	−0.83
hsa-miR-26b-5p	23,380.92	−0.41	0.00	2.77	1.16	hsa-miR-6716-3p	47.82	−0.57	0.04	−1.72	−2.98
hsa-miR-27a-5p	477.16	0.56	0.00	−2.51	0.38	hsa-miR-6847-5p	15.45	−0.82	0.03	3.04	5.06
hsa-miR-27b-5p	2,323.36	−0.34	0.04	−0.19	0.91	hsa-miR-760	345.77	−0.53	0.02	1.92	2.44
hsa-miR-301a-5p	125.21	−0.49	0.04	0.31	0.52	hsa-miR-769-5p	14,172.66	0.33	0.00	−1.18	−0.45
hsa-miR-30a-3p	1,131.05	−0.34	0.00	0.47	−0.19	hsa-miR-7974	370.02	−2.32	0.00	−2.89	−0.21
hsa-miR-30b-3p	46.79	−0.63	0.04	−0.05	1.84	hsa-miR-873-3p	1,154.19	−0.53	0.00	0.20	0.99
hsa-miR-3158-3p	118.66	0.68	0.00	0.25	−1.71	hsa-miR-887-3p	5,009.15	−0.27	0.00	0.52	−1.03
hsa-miR-3174	23.19	−0.78	0.01	−0.68	−1.61	hsa-miR-887-5p	207.56	−0.65	0.00	2.86	−0.28
hsa-miR-3176	216.31	−0.68	0.00	−3.59	−2.19	hsa-miR-92a-1-5p	180.98	−0.81	0.00	1.61	−0.55
hsa-miR-3187-3p	57.82	−0.98	0.00	−1.07	−2.69	hsa-miR-92b-5p	173.91	−0.49	0.00	0.75	1.29
hsa-miR-328-3p	528.91	0.45	0.00	−1.20	−0.95	hsa-miR-93-3p	1,166.74	−0.33	0.02	−3.47	−0.92
hsa-miR-335-3p	29.44	−0.84	0.00	−0.77	−0.82	hsa-miR-935	980.02	0.45	0.00	1.10	−0.05
						hsa-miR-98-5p	7,822.48	−0.67	0.00	−0.95	−1.18

The B score under basal conditions and following MPP$^+$ treatment is shown for each ASO targeting the corresponding deregulated miRNA. p$_{adj}$, adjusted p value.

In summary, the present study provides a catalog of protective and detrimental miRNAs with activity that affects neuronal viability, both in resting conditions and/or in response to oxidative stress. Our approach is a first step in defining druggable miRNAs in preclinical studies aiming at validating the manipulation of miRNA activity as a therapeutic strategy in neurological and neurodegenerative disorders.

MATERIALS AND METHODS
Cell Cultures
SH-SY5Y cells were grown in DMEM with L-glutamine (Biowest), supplemented with 10% inactivated fetal bovine serum (FBSi; Gibco), 1% of penicillin-streptomycin (P/S; Gibco), and 250 ng/mL of amphotericin B (Sigma-Aldrich). SH-SY5Y cells were differentiated for 4 days with retinoic acid (RA; Merck) at 10 μM and for 3 days with 12-O-tetradecanoylphorbol-13-acetate (TPA; Merck) at 80 nM. This protocol was adapted from Presgraves et al.[44] Approximately 5,000 cells were seeded per well in 96-well plates (Thermo Fisher Scientific), using a Multidrop 348 (Thermo Fisher Scientific) or in 100,000 cells in 6-well plates.

Transfection of LNA-Modified ASOs
The library consisted of 1,954 miRNA-ASOs plus 50 custom sncRNA-ASOs (Human miRCURY LNA microRNA Inhibitor Library 190103; Exiqon). Transfection was performed using a Sciclone AHL 3000 (Caliper). Briefly, 50 μL of transfection mix was added to differentiated cells grown in 100 μL of differentiation medium. The transfection mix consisted of 43.5 μL of Opti-MEM (Gibco), 0.5 μL of Lipofectamine 2000, and 6 μL of miRNA- or sncRNA-ASO. The final concentration of the ASO was 70 nM. Then, 100 μL of the transfection medium was removed 24 h later with a Platewasher ELx405 (BioTek Instruments) and replaced with 100 μL of fresh differentiation medium, with a Multidrop 348.

Each plate was transfected with 58 unique miRNA- or sncRNA-ASO, a negative mock-transfected control, and a positive control, consisting of a sncRNA-ASO with known detrimental activity. The peripheral wells were not included in the analysis and contained only medium. The 2,004 sncRNA-ASOs were distributed in 37 plates, and transfections were performed in triplicate. An additional plate was included in triplicate containing mock-transfected cells (treated only with Lipofectamine 2000; Thermo Fisher Scientific); cells transfected

with a sncRNA-ASO that does not alter cell viability, used as the negative control (miRCURY LNA Inhibitor Negative Control A; Exiqon); and cells transfected with a sncRNA-ASO, inducing cell death, used as a positive control (Custom miRCURY LNA Inhibitor Positive Control A; Exiqon). Taking into account all conditions and the replicates, the HTFS included 114 plates.

Two independent HTFSs were performed in triplicate to evaluate the effect of the miRNA- or sncRNA-ASOs in basal conditions and in response to MPP+ stress. In the HTFS under basal conditions, cell viability was determined 24 h after the addition of the fresh medium (48 h after transfection). In the HTFS aiming to evaluate the response to MPP+, the fresh medium contained MPP+ at a final concentration of 3 mM. In this case, viability was determined 24 h after treatment with MPP+ and 48 h after transfection.

MPP+ Treatment

To evaluate the involvement of miRNA- or sncRNA-ASOs in in the neuronal response to oxidative stress, cells were treated with MPP+. After differentiation and 24 h following transfection in 96-well plates, the cells were treated with a dose of MPP+ (3 mM, final concentration; Sigma-Aldrich), inducing a moderate effect on cell viability (30%–40% decrease), which was determined 24 h later.

MPP+ (3 mM) treatment was also performed in six-well plates after SHSY-5Y seeding (100,000 cells per well) and differentiation, to evaluate sncRNA perturbations occurring as a consequence of MPP+ stress.

Cell Viability Determinations

Cell viability was assessed with the WST-1 reagent[45] (Roche) 48 h after transfection. WST-1 was added to the cell medium at a ratio of 1:10. WST-1 was dispensed using a Sciclone AHL 3000. Cell plates were incubated with WST-1 at 37°C for 2 h. Then, each plate was read twice: at 440 nm and at 690 nm, using an Infinite M200 instrument (Tecan). The final absorbance value was the result of subtracting the 690 nm absorption measure from that at 440 nm and from that of a blank plate. This blank plate was also measured at 440 and 690 nm and contained growth medium without cells and WST-1 at a ratio of 1:10.

In the HTFS to evaluate the response to MPP+, a triplicate plate was added to measure the effect of MPP+ in cell viability in mock-transfected cells and in cells transfected with the sncRNA-ASO used as a positive control.

Hits Detection Based on B Score

The B score method[19] is based on the median, which is not distorted by outliers (the hits or ASOs affecting cell viability):

$$b_i = \frac{x_i - med(x)}{mad(x)}.$$

In this equation, $med(x)$ is the median of all sample values on a plate, whereas $mad(x)$ is the median absolute deviation. The numerator and denominator were adjusted to account for systematic biases. A row-column-additive model was added to the plate using the two-way median polish procedure $x_{rcp} = \mu_p + R_{rp} + C_{cp} + e_{rcp}$, where x_{rcp} is the raw value of a sample in row r, column c, and plate p. μ_p is the plate median, R_{rp} is the row effect, and C_{cp} is the column effect. Under this model, e_{rcp} is the plate-specific row-and-column-normalized value of x_{rcp}. Taking all that into account, the final B score was obtained by:

$$b'_i = \frac{e_{rcp}}{mad_p(e)}.$$

As this positional-effect-normalized B score behaves as a standardized Gaussian distribution, the hits can be defined as values below −2 (two SDs) in the screening looking at neuronal survival. In the screening related to compounds affecting viability under OS, values below −2 are considered to worsen viability in an OS context. Conversely, values above 2 in that screening indicate that the effect of the ASO is protective.

Hits Detection Based on a LMM

The previous approach was not able to deal with the variance produced by the fact that each plate was run in triplicate. Therefore, we complemented the B score approach with another one based on a LMM:

$$x_{rcpik} = \mu + R_r + C_c + \gamma_p + \alpha_i + e_{rcpik}.$$

In this equation, x_{rcpik} is the measurement value of the k-th biological replicate of the i-th compound sample in row r, column c, and plate p. μ is the overall average across all measurements. R_r and C_c are row and column fixed effects, respectively. α_i is the random effect for the i-th sample, which accounts for inter-sample variation. γ_p is the random effect for the p-th plate, which accounts for inter-plate variation. e_{rcpik} is a random-error variable, that accounts for the variability inherent to the sample. The model assumes that α_i, γ_p and e_{rcpik} are Gaussian variables with mean 0 and σ_α^2, σ_γ^2 σ_e^2 variances, respectively. Therefore, the model accounts for positional effects through the inclusion of row and column fixed effects and adds inter-plate variability. The model can easily be extended to include specific plate positional biases by the inclusion of a random effect that interacts with row and column fixed effects.

As in this approach α_i is the element of interest. The BLUP[46] (the best linear unbiased predictor of these random effects) of α_i can be used to catch samples that significantly deviate from the overall adjusted average. Because the experimental design includes biological triplicates, the model takes advantage of this by including all triplicates, instead of summarizing them, and therefore gains statistical power. In this approach, the sample outliers, the putative hits, are summarized in a single value given by the BLUPs.

ROS Quantification

Subsets of miRNA-ASOs were selected to analyze their effect on the ROS production that normally accompanies neuronal damage. miRNA-ASOs were transfected in triplicate, in six independent biological replicates. After 24 h, half of them were treated with 3 mM

MPP$^+$. CellROX Deep Red Reagent (Molecular Probes) was used to measure ROS production, and CyQUANT Direct Cell Proliferation Assay (Invitrogen) was used to normalize ROS levels by the number of cells. After the transfection (48 h), with or without treatment with MPP+ (24 h), cells were treated with CellROX Deep Red Reagent at 5 µM and incubated for 30 minutes at 37°C, and fluorescence was measured at 640/665 nm. Afterward, the same cells were treated with CyQUANT Direct Cell Proliferation Assay. CyQUANT (15 µL; 10× solution) was added to each well, the cells were incubated for 2 h at 37°C, and fluorescence was measured at 485/535 nm.

Fold change measures were used in order to assess whether the subsets of miRNA-ASOs had collective effects in the production of ROS, by comparing each subset of miRNA-ASOs affecting cell viability with the mock-transfected condition. The approach used was again a LMM, as it allowed accounting for the different sources of variability that the experiment involved. It also allowed the attainment of a normalized fold change (FC). The formula used was:

$$\log(x_{jpik}) = \mu + \beta_j + \gamma_p + \alpha_i + e_{rcpik}.$$

In this equation, x_{jpik} is the measurement value of the k-th technical replicate of the i-th miRNA-ASO in the p-th plate and the j-th group. If the miRNA-ASO affects cell viability, $j = 1$; if it does not, $j = 0$. μ is the overall average across all measurements, β_j is the group fixed effect, α_i is the random effect for the i-th miRNA-ASO (accounting for inter-miRNA-ASO variation), γ_p is the random effect for the p-th plate (accounting for inter-plate variation), and e_{jpik} is a random-error variable (accounting for the intra-sample variability). The model assumes that α_i, γ_p, and e_{rcpik} are Gaussian variables with mean 0 and σ_α^2, σ_γ^2, and σ_e^2 variances, respectively. Under the assumptions of this LMM, the adjusted FC is obtained as FC = $\exp(\beta)$.

Determination of Mitochondrial Functionality
To determine mitochondrial activity, we used the MitoTracker Deep Red probe (Invitrogen), which passively diffuses across plasma membranes and accumulates in active mitochondria. After the transfection (48 h), the cells were treated with MitoTracker Deep Red reagent at 0.1 µM and incubated for 1 h at 37°C, and fluorescence was measured at 579/599 nm. Carbonylcyanide chlorophenylhydrazone (CCCP) 5 mM was used as the positive control for the mitochondria depolarization. The Kruskal-Wallis test was used to compare all conditions, followed by the Mann-Whitney U test with Bonferroni's post hoc correction. p < 0.05 was considered statistically significant.

RNA Extraction and Small RNA Sequencing
Total RNA was isolated from cells, 24 h after treatment with MPP+ or a control solution, in four independent biological replicates. After the medium was removed from cells treated with MPP+ for 24 h, the plates were washed once in PBS and immediately frozen at −80°C. Total RNA was isolated with the miRNeasy kit (QIAGEN), according to the manufacturer's instructions.

RNA integrity was evaluated with Bioanalyzer 2100 (Applied Biosystems), with RNA integrity number (RIN) > 9 in all samples. Small RNA (sRNA) indexed libraries for sequencing were prepared from 1 µg of total RNA, using the Trueseq kit (Illumina), according to the manufacturer's specifications. Library preparation for control and MPP+-treated cells was performed in parallel, and indexed samples were sequenced in a single lane in a HiSeq2000 (Illumina). The reads generated were 50 nt long.

sRNA Profiling
Reads were trimmed to 36 nt and ligation adapters removed using the adrec.jar program from the seqBuster suite.[47] Sequences were mapped to the hg19 genome. sRNA processing, mapping, and annotation were performed using the SeqBuster and SeqCluster tools, as described in prior studies.[47,48] We used DESeq2 for differential expression analysis and log$_2$ transformation of the count data. We followed the standard steps for the analysis: load count matrix, estimation of dispersion, and negative binomial Wald test, with outlier removal using DESeq2 functions.[49]

SUPPLEMENTAL INFORMATION
Supplemental Information can be found online at https://doi.org/10.1016/j.omtn.2019.06.007.

AUTHOR CONTRIBUTIONS

CONFLICTS OF INTEREST
The authors declare no competing interests.

ACKNOWLEDGMENTS

REFERENCES
1. Treiber, T., Treiber, N., and Meister, G. (2019). Regulation of microRNA biogenesis and its crosstalk with other cellular pathways. Nat. Rev. Mol. Cell Biol. 20, 5–20.

2. Bartel, D.P. (2009). MicroRNAs: target recognition and regulatory functions. Cell 136, 215–233.

3. Friedman, R.C., Farh, K.K.H., Burge, C.B., and Bartel, D.P. (2009). Most mammalian mRNAs are conserved targets of microRNAs. Genome Res. 19, 92–105.

4. Friedländer, M.R., Lizano, E., Houben, A.J.S., Bezdan, D., Báñez-Coronel, M., Kudla, G., Mateu-Huertas, E., Kagerbauer, B., González, J., Chen, K.C., et al. (2014). Evidence for the biogenesis of more than 1,000 novel human microRNAs. Genome Biol. 15, R57.

5. Cao, X., Yeo, G., Muotri, A.R., Kuwabara, T., and Gage, F.H. (2006). Noncoding RNAs in the mammalian central nervous system. Annu. Rev. Neurosci. 29, 77–103.

6. Li, X., and Jin, P. (2010). Roles of small regulatory RNAs in determining neuronal identity. Nat. Rev. Neurosci. 11, 329–338.

7. Davis, T.H., Cuellar, T.L., Koch, S.M., Barker, A.J., Harfe, B.D., McManus, M.T., and Ullian, E.M. (2008). Conditional loss of Dicer disrupts cellular and tissue morphogenesis in the cortex and hippocampus. J. Neurosci. 28, 4322–4330.

8. Kim, J., Inoue, K., Ishii, J., Vanti, W.B., Voronov, S.V., Murchison, E., Hannon, G., and Abeliovich, A. (2007). A MicroRNA feedback circuit in midbrain dopamine neurons. Science 317, 1220–1224.

9. McLoughlin, H.S., Fineberg, S.K., Ghosh, L.L., Tecedor, L., and Davidson, B.L. (2012). Dicer is required for proliferation, viability, migration and differentiation in cortico-neurogenesis. Neuroscience 223, 285–295.

10. Miñones-Moyano, E., Porta, S., Escaramís, G., Rabionet, R., Iraola, S., Kagerbauer, B., Espinosa-Parrilla, Y., Ferrer, I., Estivill, X., and Martí, E. (2011). MicroRNA profiling of Parkinson's disease brains identifies early downregulation of miR-34b/c which modulate mitochondrial function. Hum. Mol. Genet. 20, 3067–3078.

11. Miñones-Moyano, E., Friedländer, M.R., Pallares, J., Kagerbauer, B., Porta, S., Escaramís, G., Ferrer, I., Estivill, X., and Martí, E. (2013). Upregulation of a small vault RNA (svtRNA2-1a) is an early event in Parkinson disease and induces neuronal dysfunction. RNA Biol. 10, 1093–1106.

12. Absalon, S., Kochanek, D.M., Raghavan, V., and Krichevsky, A.M. (2013). MiR-26b, upregulated in Alzheimer's disease, activates cell cycle entry, tau-phosphorylation, and apoptosis in postmitotic neurons. J. Neurosci. 33, 14645–14659.

13. Yang, J., Brown, M.E., Zhang, H., Martinez, M., Zhao, Z., Bhutani, S., Yin, S., Trac, D., Xi, J.J., and Davis, M.E. (2017). High-throughput screening identifies microRNAs that target Nox2 and improve function after acute myocardial infarction. Am. J. Physiol. Heart Circ. Physiol. 312, H1002–H1012.

14. Van Peer, G., Mets, E., Claeys, S., De Punt, I., Lefever, S., Ongenaert, M., Rondou, P., Speleman, F., Mestdagh, P., and Vandesompele, J. (2018). A high-throughput 3′ UTR reporter screening identifies microRNA interactomes of cancer genes. PLoS ONE 13, e0194017.

15. Drakaki, A., Hatziapostolou, M., Polytarchou, C., Vorvis, C., Poultsides, G.A., Souglakos, J., Georgoulias, V., and Iliopoulos, D. (2015). Functional microRNA high throughput screening reveals miR-9 as a central regulator of liver oncogenesis by affecting the PPARA-CDH1 pathway. BMC Cancer 15, 542.

16. Cunha, P.P., Costa, P.M., Morais, C.M., Lopes, I.R., Cardoso, A.M., Cardoso, A.L., Mano, M., Jurado, A.S., and Pedroso de Lima, M.C. (2017). High-throughput screening uncovers miRNAs enhancing glioblastoma cell susceptibility to tyrosine kinase inhibitors. Hum. Mol. Genet. 26, 4375–4387.

17. Yuan, Y., Niu, F., Nolte, I.M., Koerts, J., de Jong, D., Rutgers, B., Osinga, J., Azkanaz, M., Terpstra, M., Bystrykh, L., et al. (2018). MicroRNA High Throughput Loss-of-Function Screening Reveals an Oncogenic Role for miR-21-5p in Hodgkin Lymphoma. Cell. Physiol. Biochem. 49, 144–159.

18. Soriano, A., Masanas, M., Boloix, A., Masiá, N., París-Coderch, L., Piskareva, O., Jiménez, C., Henrich, K.O., Roma, J., Westermann, F., et al. (2019). Functional high-throughput screening reveals miR-323a-5p and miR-342-5p as new tumor-suppressive microRNA for neuroblastoma. Cell. Mol. Life Sci. 76, 2231–2243.

19. Brideau, C., Gunter, B., Pikounis, B., and Liaw, A. (2003). Improved statistical methods for hit selection in high-throughput screening. J. Biomol. Screen. 8, 634–647.

20. Pantano, L., Friedländer, M.R., Escaramís, G., Lizano, E., Pallarès-Albanell, J., Ferrer, I., Estivill, X., and Martí, E. (2016). Specific small-RNA signatures in the amygdala at premotor and motor stages of Parkinson's disease revealed by deep sequencing analysis. Bioinformatics 32, 673–681.

21. Xicoy, H., Wieringa, B., and Martens, G.J.M. (2017). The SH-SY5Y cell line in Parkinson's disease research: a systematic review. Mol. Neurodegener. 12, 10.

22. Kovalevich, J., and Langford, D. (2013). Considerations for the use of SH-SY5Y neuroblastoma cells in neurobiology. Methods Mol. Biol. 1078, 9–21.

23. Ishiyama, M., Tominaga, H., Shiga, M., Sasamoto, K., Ohkura, Y., and Ueno, K. (1996). A combined assay of cell viability and in vitro cytotoxicity with a highly water-soluble tetrazolium salt, neutral red and crystal violet. Biol. Pharm. Bull. 19, 1518–1520.

24. Backes, C., Khaleeq, Q.T., Meese, E., and Keller, A. (2016). miEAA: microRNA enrichment analysis and annotation. Nucleic Acids Res. 44,, W110–W116.

25. Schneider, R., McKeever, P., Kim, T., Graff, C., van Swieten, J.C., Karydas, A., Boxer, A., Rosen, H., Miller, B.L., Laforce, R., Jr., et al.; Genetic FTD Initiative (GENFI) (2018). Downregulation of exosomal miR-204-5p and miR-632 as a biomarker for FTD: a GENFI study. J. Neurol. Neurosurg. Psychiatry 89, 851–858.

26. Palm, T., Bahnassawy, L., and Schwamborn, J. (2012). MiRNAs and neural stem cells: a team to treat Parkinson's disease? RNA Biol. 9, 720–730.

27. Briggs, C.E., Wang, Y., Kong, B., Woo, T.-U.W., Iyer, L.K., and Sonntag, K.C. (2015). Midbrain dopamine neurons in Parkinson's disease exhibit a dysregulated miRNA and target-gene network. Brain Res. 1618, 111–121.

28. Moreau, M.P., Bruse, S.E., David-Rus, R., Buyske, S., and Brzustowicz, L.M. (2011). Altered microRNA expression profiles in postmortem brain samples from individuals with schizophrenia and bipolar disorder. Biol. Psychiatry 69, 188–193.

29. Tang, Y., Ling, Z.M., Fu, R., Li, Y.Q., Cheng, X., Song, F.H., Luo, H.X., and Zhou, L.H. (2014). Time-specific microRNA changes during spinal motoneuron degeneration in adult rats following unilateral brachial plexus root avulsion: ipsilateral vs. contralateral changes. BMC Neurosci. 15, 92.

30. Stark, K.L., Xu, B., Bagchi, A., Lai, W.-S., Liu, H., Hsu, R., Wan, X., Pavlidis, P., Mills, A.A., Karayiorgou, M., and Gogos, J.A. (2008). Altered brain microRNA biogenesis contributes to phenotypic deficits in a 22q11-deletion mouse model. Nat. Genet. 40, 751–760.

31. Santarelli, D.M., Beveridge, N.J., Tooney, P.A., and Cairns, M.J. (2011). Upregulation of dicer and microRNA expression in the dorsolateral prefrontal cortex Brodmann area 46 in schizophrenia. Biol. Psychiatry 69, 180–187.

32. Pons-Espinal, M., de Luca, E., Marzi, M.J., Beckervordersandforth, R., Armirotti, A., Nicassio, F., Fabel, K., Kempermann, G., and De Pietri Tonelli, D. (2017). Synergic Functions of miRNAs Determine Neuronal Fate of Adult Neural Stem Cells. Stem Cell Reports 8, 1046–1061.

33. Stappert, L., Borghese, L., Roese-Koerner, B., Weinhold, S., Koch, P., Terstegge, S., Uhrberg, M., Wernet, P., and Brüstle, O. (2013). MicroRNA-based promotion of human neuronal differentiation and subtype specification. PLoS ONE 8, e59011.

34. Sasaki, Y., Gross, C., Xing, L., Goshima, Y., and Bassell, G.J. (2014). Identification of axon-enriched microRNAs localized to growth cones of cortical neurons. Dev. Neurobiol. 74, 397–406.

35. Owczarzy, R., You, Y., Groth, C.L., and Tataurov, A.V. (2011). Stability and mismatch discrimination of locked nucleic acid-DNA duplexes. Biochemistry 50, 9352–9367.

36. Cheng, A.M., Byrom, M.W., Shelton, J., and Ford, L.P. (2005). Antisense inhibition of human miRNAs and indications for an involvement of miRNA in cell growth and apoptosis. Nucleic Acids Res. 33, 1290–1297.

37. Du, L., Borkowski, R., Zhao, Z., Ma, X., Yu, X., Xie, X.-J., and Pertsemlidis, A. (2013). A high-throughput screen identifies miRNA inhibitors regulating lung cancer cell survival and response to paclitaxel. RNA Biol. 10, 1700–1713.

38. Chakrabarti, M., Banik, N.L., and Ray, S.K. (2014). MiR-7-1 potentiated estrogen receptor agonists for functional neuroprotection in VSC4.1 motoneurons. Neuroscience 256, 322–333.

39. Huang, W., Liu, X., Cao, J., Meng, F., Li, M., Chen, B., and Zhang, J. (2015). miR-134 regulates ischemia/reperfusion injury-induced neuronal cell death by regulating CREB signaling. J. Mol. Neurosci. 55, 821–829.

40. Sabirzhanov, B., Zhao, Z., Stoica, B.A., Loane, D.J., Wu, J., Borroto, C., Dorsey, S.G., and Faden, A.I. (2014). Downregulation of miR-23a and miR-27a following experimental traumatic brain injury induces neuronal cell death through activation of proapoptotic Bcl-2 proteins. J. Neurosci. 34, 10055–10071.

41. Fragkouli, A., and Doxakis, E. (2014). miR-7 and miR-153 protect neurons against MPP(+)-induced cell death via upregulation of mTOR pathway. Front. Cell. Neurosci. 8, 182.

42. Moon, J.M., Xu, L., and Giffard, R.G. (2013). Inhibition of microRNA-181 reduces forebrain ischemia-induced neuronal loss. J. Cereb. Blood Flow Metab. 33, 1976–1982.

43. Khanna, S., Rink, C., Ghoorkhanian, R., Gnyawali, S., Heigel, M., Wijesinghe, D.S., Chalfant, C.E., Chan, Y.C., Banerjee, J., Huang, Y., et al. (2013). Loss of miR-29b following acute ischemic stroke contributes to neural cell death and infarct size. J. Cereb. Blood Flow Metab. 33, 1197–1206.

44. Presgraves, S.P., Ahmed, T., Borwege, S., and Joyce, J.N. (2004). Terminally differentiated SH-SY5Y cells provide a model system for studying neuroprotective effects of dopamine agonists. Neurotox. Res. 5, 579–598.

45. Berridge, M.V., Herst, P.M., and Tan, A.S. (2005). Tetrazolium dyes as tools in cell biology: new insights into their cellular reduction. Biotechnol. Annu. Rev. 11, 127–152.

46. Robinson, G.K. (1991). That BLUP is a good thing: the estimation of random effects. Stat. Sci. 6, 15–32.

47. Pantano, L., Estivill, X., and Martí, E. (2010). SeqBuster, a bioinformatic tool for the processing and analysis of small RNAs datasets, reveals ubiquitous miRNA modifications in human embryonic cells. Nucleic Acids Res. 38, e34.

48. Pantano, L., Estivill, X., and Martí, E. (2011). A non-biased framework for the annotation and classification of the non-miRNA small RNA transcriptome. Bioinformatics 27, 3202–3203.

49. Love, M.I., Huber, W., and Anders, S. (2014). Moderated estimation of fold change and dispersion for RNA-seq data with DESeq2. Genome Biol. 15, 550.